Structural Eng. / Earthquake Eng. Vol. 6. No. 1, 141s-150s. April 1989
Japan Society of Civil Engineers (Proc. of JSCE No. 404/I-11)

STUDY ON RESPONSE OF BURIED PIPELINES SUBJECTED TO LIQUEFACTION-INDUCED PERMANENT GROUND DISPLACEMENT

By Masakatsu MIYAJIMA, Masaru KITAURA** and Yoshinori NOMURA****

The present paper deals with the response of pipelines subjected to liquefaction-induced permanent ground displacement and the subsequent failure of pipelines is discussed. Initially here, characteristics of permanent ground displacement are investigated based on model experiments. Next, formulae obtained by a beam theory are established and preliminary analysis is carried out in order to understand fundamental characteristics of continuous pipelines. Furthermore, response simulations are conducted for jointed pipelines by using a modified transfer matrix method. We present the influential factors determining the magnitude of the ground displacements and propose the method for evaluation of pipeline response to permanent ground displacement.

Keywords : buried pipeline, liquefaction, model experiment, permanent ground displacement

1. INTRODUCTION

Permanent ground displacement induced by soil liquefaction is one of the most serious liquefaction hazards. Using aerial photographs taken before and just after the earthquakes, Hamada et al. measured the permanent ground displacement following the 1964 Niigata Earthquake and the 1983 Nipponkai-Chubu Earthquake. According to their findings, the maximum detected permanent ground displacement was more than 8 m along the Shinano river in Niigata City and more than 5 m in Noshiro City[1]. They also analyzed the quantitative correlations of the magnitude of the permanent ground displacement with the degree of damage to pipelines[2]. We investigated the relationship between permanent ground displacement and pipeline damage following the 1983 Nipponkai-Chubu Earthquake. The main points of interest were as follows : Most of the permanent ground displacement, exceeding 1 m, occurred in the liquefied areas and the damage ratios of the pipelines were also high in those areas[3]. O'Rourke and Tawfik investigated pipeline response to permanent ground displacement near the Upper Van Norman Reservoir after the 1971 San Fernando Earthquake and related the damage to the patterns of permanent ground movement[4]. These results indicated that buried pipelines were vulnerable to permanent ground deformation. Furthermore, Yasuda et al. carried out model experiments considering the characteristics of permanent ground displacement and discussed the causes of permanent ground displacement[5]. Little work has been done on the response of pipelines subjected to permanent ground deformation so far, however.

The purposes of the present study are to clarify the response of pipelines subjected to liquefaction-

* Member of JSCE, M. Eng., Assistant Professor, Department of Civil Engineering, Kanazawa University (2-40-20, Kodatsuno, Kanazawa, Ishikawa).
** Member of JSCE, Dr. Eng., Professor, ditto.
*** Member of JSCE, M. Eng., Engineer, Fukui Prefectural Government.

induced permanent ground displacement and to discuss the subsequent failure of pipelines. In the following Chapter 2, characteristics of permanent ground displacement are investigated based on model experiments. In Chapter 3, formulae obtained by a beam theory are described and preliminary analysis is carried out in order to obtain fundamental characteristics of continuous pipelines. Moreover, response simulations are performed by using a modified transfer matrix method and failures of jointed pipelines due to liquefaction-induced permanent ground deformation are discussed in Chapter 4. The results obtained from the present study can give us a useful piece of information for determining whether or not countermeasures for the pipeline buried in the ground with high liquefaction potential should be taken, and what countermeasures should be done.

2. EXPERIMENTS ON LIQUEFACTION-INDUCED PERMANENT GROUND DISPLACEMENT

The distribution of permanent ground displacement along pipelines and magnification of the displacement are crucial factors in analysis of pipeline response. According to a distribution map of permanent ground displacement resulting from the 1964 Niigata Earthquake and the 1983 Nipponkai-Chubu Earthquake indicated by Hamada et al.[1], the distribution of permanent ground displacement is affected by local ground conditions such as the ground surface, the depth of the liquefied ground layer, etc. In this chapter, model experiments are carried out to understand the characteristics of the permanent ground displacement.

(1) Testing procedure

The diagram of the experimental apparatus is shown in Fig. 1. The sand box was 500 mm in width, 1 500 mm in length and 350 mm in height. The model sand deposit had a slope θ of 2 % to 6 %. The sand deposit was made from loose saturated sand, whose physical properties are shown in Table 1. Since the sand stratum was constructed in water in these experiments, whole sand stratum was saturated and the ground water table depth did not vary for each case. Therefore the effects of the ground water table depth were negligible in these experiments. Forty six pins were installed at the surface of the sand stratum to measure horizontal deformation of the ground surface. The deformation of the ground surface during excitation was measured by means of a video camera. Pore pressure transducers were buried to a depth of 5 cm to measure an excess pore water pressure in the loose sand stratum and in the more dense one. The model sand stratum was vibrated by a harmonic wave with 5 Hz. Target acceleration of the table was 100 gal and it took about 5 seconds for the table to reach the given acceleration. The duration of the test was 30 seconds.

(2) Experimental results and discussion

Fig. 2 shows the time histories of input acceleration, excess pore water pressure at the loose sand

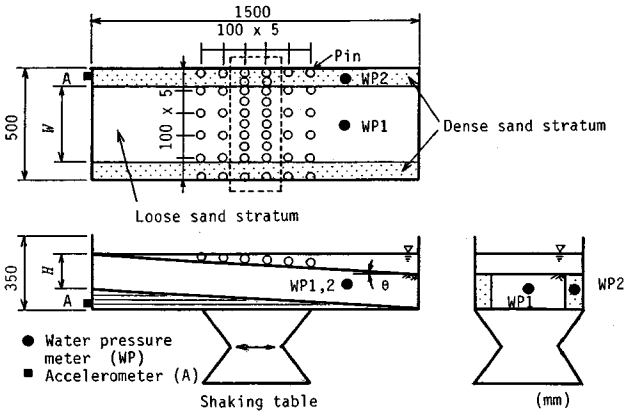

Fig. 1 General view of experimental apparatus.

Table 1 Physical properties of sand.

Specific gravity	2.67
Uniformity coefficient	2.96
Maximum void ratio	1.030
Minimum void ratio	0.721
50 percent diameter (mm)	0.2
Coefficient of permeability (cm/s)	0.0192

stratum (WP 1) and displacement at point 7 which is shown in Fig. 4 as described later. It is evident from this figure that the model ground deformed in high excess pore water pressure, that is, in a completely liquefied condition. Fig. 3 shows distribution of the permanent ground displacement. It is interesting to note that the ground displacement in the middle of the loose sand stratum was greater than that at the sides and the dense sand stratum did not defrom. Since the wall of the sand box was against deformation of the sand stratum, the ground displacement in the loose sand stratum near the wall was also little. Therefore, the experiments carried out in the present study corresponded with the permanent ground displacement when liquefaction uniformly occurred in a certain area, which was enclosed with the dense sand stratum and two walls of the sand box in this experiment. Fig. 4 reflects distribution of residual permanent ground displacement at the middle of the ground surface, shown inside of the dashed area in Fig. 1. In this figure, the open circles indicate the initial sites of the pins and the solid circles, squares and triangles show the residual displacement of the pins for each case. This figure suggests that the shape of the distribution of the permanent ground displacement is approximately a sinusoidal curve. Furthermore, the maximum value of the permanent ground displacement is affected by the width of the loose sand deposit, W. Fig. 5 shows

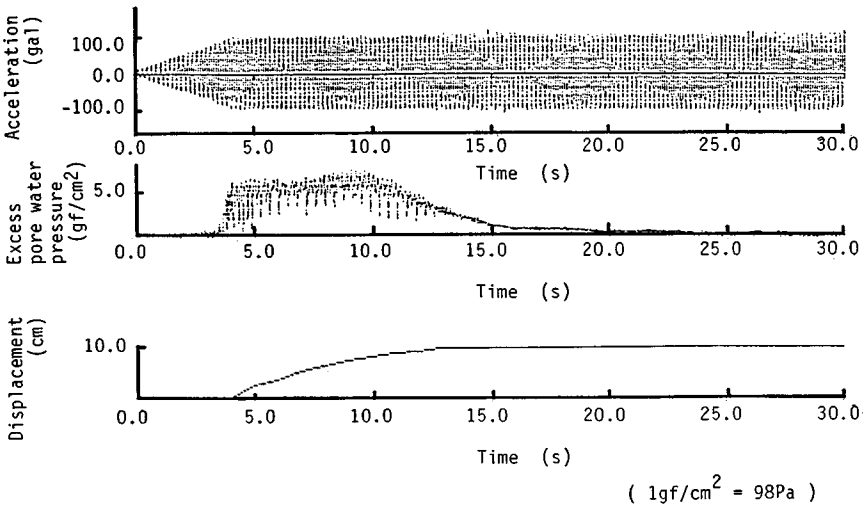

Fig. 2 Time histories of input acceleration, excess pore water pressure (WP 1), and displacement at point 7.

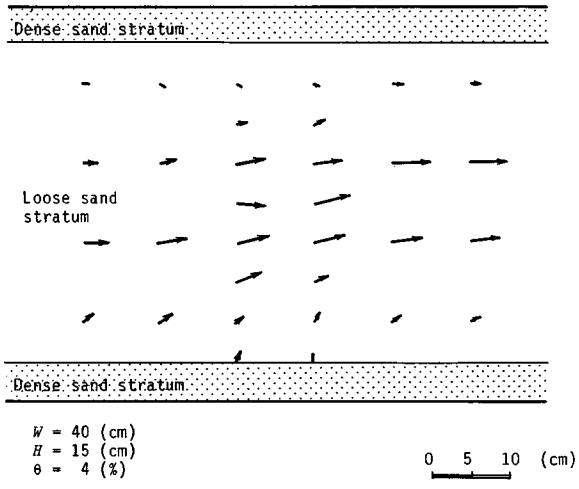

Fig. 3 Distribution of permanent ground displacement.

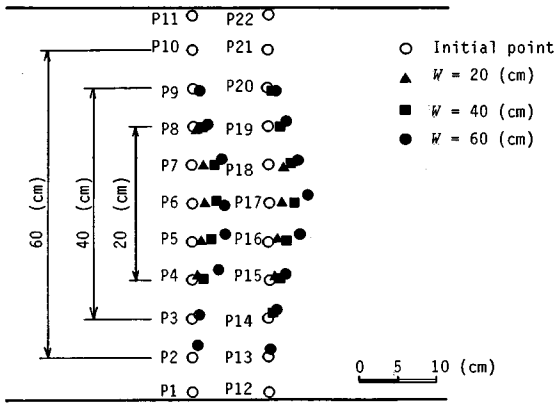

Fig. 4 Distribution of residual permanent ground displacement.

the relationship between the width of the loose sand stratum and the maximum value of the permanent ground displacement. The maximum value seems to be directly proportional to the width of the loose sand deposit.

Hamada et al. proposed a formula for estimating the magnitude of ground displacement by using the data obtained from the 1964 Niigata, the 1971 San Fernando, and the 1983 Nipponkai-Chubu Earthquakes[2]. In this formula, the ground slope and thickness of the liquefied layer were taken into consideration. Our experimental results mentioned above, however, suggest that the width of permanent ground displacement is one of the influential factors determining the magnitude of the ground displacements; moreover, the distribution of the permanent ground displacement, which is one of the crucial factors in analysis of pipeline response, displayed a sinusoidal curve.

3. DESIGN FORMULAE AND PRELIMINARY ANALYSIS

(1) Formulae for analyzing response of pipelines due to permanent ground displacement

The distribution of the permanent ground displacement can be assumed to be a sinusoidal curve as mentioned in the previous chapter. Although the results of the experiments indicate one of the displacement patterns which depend on the several ground conditions, this pattern is considered as the basic pattern of the ground displacement. It is because this pattern is shown when liquefaction uniformly occurred in the loose sand stratum on smooth slope of the non-liquefied ground. The displacement pattern in this case is modeled as shown in Fig. 6. The basic differential equations governing the motion of a buried pipe can be established as follows:

a) $0 \leqq x < l$

$$EI\frac{d^4v_1}{dx^4}+K_1v_1=K_1\delta\left(1-\sin\frac{\pi x}{2l}\right) \quad \cdots\cdots (1)$$

b) $l \leqq x$

$$EI\frac{d^4v_2}{dx^4}+K_2v_2=0 \quad \cdots\cdots (2)$$

where E=Young's modulus of the pipe material, I=area moment of inertia of the pipe, v_1, v_2= displacements of pipeline at each zone, K_1, K_2=equivalent soil spring constants for deformed ground and non-deformed ground, which depend on the degree of liquefaction of the soil, δ=the maximum magnitude of the permanent ground displacement and l=half of extent of the permanent ground displacement along the pipeline, that is, $2l=W$. Boundary conditions are given as follows:

a) at $x=0$, $\dfrac{dv_1}{dx}=0$, $\dfrac{d^3v_1}{dx^3}=0$ $\cdots\cdots (3)$

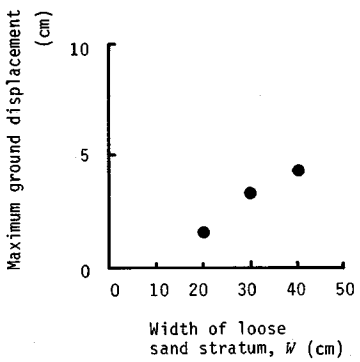

Fig. 5 Relationship between width of loose sand stratum and maximum ground displacement.

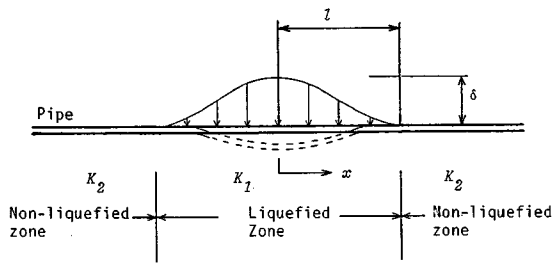

Fig. 6 Analytical model (Plane figure).

Table 2 v_0 and constants in integration.

$$v_0 = \delta - D_0 \sin\frac{\pi x}{2l}$$

$$A_1 = \frac{B_{17}C_1 - B_{18}C_2 + B_{19}C_3 - B_{20}C_4}{B_1C_1 - B_2C_2 + B_3C_3 - B_4C_4}$$

$$A_2 = \frac{-B_{17}C_5 + B_{18}C_6 - B_{19}C_7 + B_{20}C_8}{-B_5C_5 + B_6C_6 - B_7C_7 + B_8C_8}$$

$$A_3 = F_1 + A_1$$

$$A_4 = F_2 - A_2$$

$$A_5 = \frac{B_{17}C_9 - B_{18}C_{10} + B_{19}C_{11} - B_{20}C_{12}}{B_9C_9 - B_{10}C_{10} + B_{11}C_{11} - B_{12}C_{12}}$$

$$A_6 = \frac{-B_{17}C_{13} + B_{18}C_{14} - B_{19}C_{15} + B_{20}C_{16}}{-B_{13}C_{13} + B_{14}C_{14} - B_{15}C_{15} + B_{16}C_{16}}$$

$$B_1 = (\exp(\beta_1 l) + \exp(-\beta_1 l))\cos\beta_1 l$$

$$B_2 = D_5(D_2\exp(\beta_1 l) - D_1\exp(-\beta_1 l))$$

$$B_3 = D_5^2(-\exp(\beta_1 l) + \exp(-\beta_1 l))\sin\beta_1 l$$

$$B_4 = D_5^3(-D_1\exp(\beta_1 l) + D_2\exp(-\beta_1 l))$$

$$B_5 = (\exp(\beta_1 l) - \exp(-\beta_1 l))\sin\beta_1 l$$

$$B_6 = D_5(D_1\exp(\beta_1 l) - D_2\exp(-\beta_1 l))$$

$$B_7 = D_5^2(\exp(\beta_1 l) + \exp(-\beta_1 l))\cos\beta_1 l$$

$$B_8 = D_5^3(D_2\exp(\beta_1 l) - D_1\exp(-\beta_1 l))$$

$$B_9 = -\exp(-\beta_2 l)\cos\beta_2 l$$

$$B_{10} = D_3\exp(-\beta_2 l)$$

$$B_{11} = -\exp(-\beta_2 l)\sin\beta_2 l$$

$$B_{12} = -D_4\exp(-\beta_2 l)$$

$$B_{13} = B_{11}$$

$$B_{14} = B_{12}$$

$$B_{15} = -B_9$$

$$B_{16} = -B_{10}$$

$$B_{17} = -\exp(-\beta_1 l)(F_1\cos\beta_1 l + F_2\sin\beta_1 l) - \frac{EI}{K_1}\left(\frac{\pi}{2l}\right)^4 D_0$$

$$B_{18} = D_5\exp(-\beta_1 l)(F_1D_1 - F_2D_2)$$

$$B_{19} = D_5^2\exp(-\beta_1 l)(-F_1\sin\beta_1 l + F_2\cos\beta_1 l) - \frac{1}{2}\left(\frac{\pi}{2l\beta_2}\right)^2 D_0$$

$$B_{20} = -D_5^3\exp(-\beta_1 l)(F_1D_2 + F_2D_1)$$

$$C_1 = B_6B_{11}B_{16} + B_{10}B_{15}B_8 + B_{14}B_{12}B_7 - B_{14}B_{11}B_8 - B_6B_{12}B_{15} - B_{10}B_7B_{16}$$

$$C_2 = B_5B_{11}B_{16} + B_9B_{15}B_8 + B_{13}B_{12}B_7 - B_{13}B_{11}B_8 - B_5B_{12}B_{15} - B_9B_7B_{16}$$

$$C_3 = B_5B_{10}B_{16} + B_9B_{14}B_8 + B_{13}B_{12}B_6 - B_{13}B_{10}B_8 - B_5B_{12}B_{14} - B_9B_6B_{16}$$

$$C_4 = B_5B_{10}B_{15} + B_9B_{14}B_7 + B_{13}B_{11}B_6 - B_{13}B_{10}B_7 - B_5B_{11}B_{14} - B_9B_6B_{15}$$

$$C_5 = B_2B_{11}B_{16} + B_{10}B_{15}B_4 + B_{14}B_{12}B_3 - B_{14}B_{11}B_4 - B_{10}B_3B_{16} - B_2B_{12}B_{15}$$

$$C_6 = B_1B_{11}B_{16} + B_9B_{15}B_4 + B_{13}B_{12}B_3 - B_{13}B_{11}B_4 - B_9B_3B_{16} - B_1B_{12}B_{15}$$

$$C_7 = B_1B_{10}B_{16} + B_9B_{14}B_4 + B_{13}B_{12}B_2 - B_{13}B_{10}B_4 - B_9B_2B_{16} - B_1B_{12}B_{14}$$

$$C_8 = B_1B_{10}B_{15} + B_9B_{14}B_3 + B_{13}B_{11}B_2 - B_{13}B_{10}B_3 - B_9B_2B_{15} - B_1B_{11}B_{14}$$

$$C_9 = B_2B_7B_{16} + B_6B_{15}B_4 + B_{14}B_8B_3 - B_{14}B_7B_4 - B_2B_8B_{15} - B_6B_3B_{16}$$

$$C_{10} = B_1B_7B_{16} + B_5B_{15}B_4 + B_{13}B_8B_3 - B_{13}B_7B_4 - B_1B_8B_{15} - B_5B_3B_{16}$$

$$C_{11} = B_1B_6B_{16} + B_5B_{14}B_4 + B_{13}B_8B_2 - B_{13}B_6B_4 - B_1B_8B_{14} - B_5B_2B_{16}$$

$$C_{12} = B_1B_6B_{15} + B_5B_{14}B_3 + B_{13}B_7B_2 - B_{13}B_6B_3 - B_1B_7B_{14} - B_5B_2B_{15}$$

$$C_{13} = B_2B_7B_{12} + B_{10}B_8B_3 + B_6B_{11}B_4 - B_{10}B_7B_4 - B_2B_8B_{11} - B_6B_3B_{12}$$

$$C_{14} = B_1B_7B_{12} + B_9B_8B_3 + B_5B_{11}B_4 - B_9B_7B_4 - B_1B_8B_{11} - B_5B_3B_{12}$$

$$C_{15} = B_1B_6B_{12} + B_9B_8B_2 + B_5B_{10}B_4 - B_9B_6B_4 - B_1B_8B_{10} - B_5B_2B_{12}$$

$$C_{16} = B_1B_6B_{11} + B_9B_7B_2 + B_5B_{10}B_3 - B_9B_6B_3 - B_1B_7B_{10} - B_5B_2B_{11}$$

$$D_0 = \frac{\delta}{1 + \frac{EI}{K_1}\left(\frac{\pi}{2l}\right)^4}$$

$$D_1 = \cos\beta_1 l + \sin\beta_1 l$$

$$D_2 = \cos\beta_1 l - \sin\beta_1 l$$

$$D_3 = \cos\beta_2 l + \sin\beta_2 l$$

$$D_4 = \cos\beta_2 l - \sin\beta_2 l$$

$$D_5 = \frac{\beta_1}{\beta_2}$$

$$F_1 = -\frac{\pi}{4\beta_1 l}\left\{1 + \frac{1}{2\beta_1^2}\left(\frac{\pi}{2l}\right)^2\right\} D_0$$

$$F_2 = \frac{\pi}{4\beta_1 l}\left\{1 - \frac{1}{2\beta_1^2}\left(\frac{\pi}{2l}\right)^2\right\} D_0$$

b) at $x=l$, $v_1=v_2$, $\frac{dv_1}{dx}=\frac{dv_2}{dx}$, $\frac{d^2v_1}{dx^2}=\frac{d^2v_2}{dx^2}$, $\frac{d^3v_1}{dx^3}=\frac{d^3v_2}{dx^3}$ ..... (4)

c) at $x\to\infty$, $v_2=0$, $\frac{dv_2}{dx}=0$ ..... (5)

Solving the equations by use of the boundary conditions, displacements of the pipe are obtained as follows :

$$v_1=\exp(\beta_1 x)(A_1\cos\beta_1 x+A_2\sin\beta_1 x)+\exp(-\beta_1 x)(A_3\cos\beta_1 x+A_4\sin\beta_1 x)+v_0 \quad \cdots\cdots (6)$$

$$v_2=\exp(-\beta_2 x)(A_5\cos\beta_2 x+A_6\sin\beta_2 x) \quad \cdots\cdots (7)$$

In these equations, v_0 and $A_1\sim A_6$, which are constants in integration, are presented in Table 2, $\beta_1^4=K_1/(4EI)$ and $\beta_2^4=K_2/(4EI)$.

(2) Application of these formulae to existing ground and pipelines

Fig. 7 shows the relationship between the maximum bending pipe stress and width of the liquefied zone as shown in Fig. 6. The maximum magnitude of the permanent ground displacement is 1 m in this case. The pipelines used in this analysis are continuous steel pipelines, whose dimensions are shown in Table 3. The pipelines with this size are usually used as the main distribution pipelines for water service. It can be seen from this figure that the smaller the ratio of the equivalent spring constant, K_1/K_2 becomes, in other words, the higher the degree of liquefaction, the smaller the maximum bending pipe stress. It can be explained in terms of decrease in the force due to ground deformation acting on the pipelines and the slippage between the pipelines and the liquefied ground. The maximum bending stress for $K_1/K_2=1.0$ becomes greater than the allowable bending stress of the steel pipeline, (4 200 kgf/cm^2 (411.6 MPa)) at a width of the liqufied ground less than about 150 m except for the region near to 0 m of the width in this example; therefore the probability of pipe failure is markedly high in cases of greater ratio of the equivalent soil spring constant. It is also interesting to note that the response of pipelines did not vary remarkably in case of greater than 300 m width of liquefied ground. These findings suggest that the response of pipelines subjected to permanent ground displacement is very sensitive to the equivalent soil spring constant. The equivalent soil spring constant for liquefiable ground depends on the degree of liquefaction of the soil. Yoshida et al. carried out experiments using a model pile in the liquefied ground and indicated that the coefficient of subgrade reaction on pile decreased to 1 percent or more of that in the non-liquefied ground[6]. Takada et al., after conducting model experiments to obtain the equivalent soil spring constant of the pipeline in the liquefied ground, pointed out that the ratio of 1/1 000 to 1/3 000 seems to be an appropriate value adopted for the buried pipeline subjected to liquefaction[7]. Yasuda et al. also conducted experiments using sand box and steel pipe, and concluded that critical shearing force and equivalent soil spring constant in the liquefied ground became less than 10 percent of those in the non-liquefied ground[8]. Although some experimental results are revealed as mentioned above, accumulation

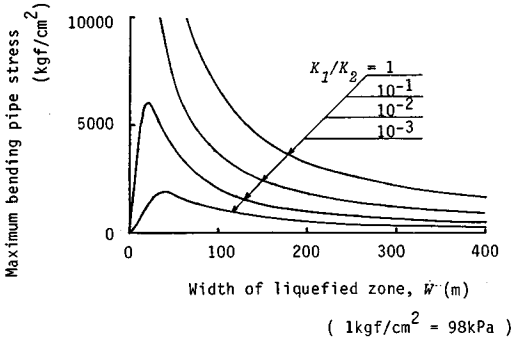

Fig. 7 Relationship between width of liquefied zone and maximum bending pipe stress.

Table 3 Dimensions of pipes.

		SP	DCIP
Outer diameter	(mm)	406.4	425.6
Thickness	(mm)	6.0	8.5
Young's modulus	(kgf/cm^2)	2.1 x10^6	1.6 x10^6
Specific gravity		7.85	7.15

SP : Steel pipe
DCIP : Ductile cast iron pipe
(1kgf/cm^2 = 98kPa)

of experimental data under various conditions is inevitable before these values are used in the earthquake resistant design. Therefore, the equivalent soil spring constant is regarded as a variable in the present study.

4. SIMULATION OF PIPELINES' RESPONSE DUE TO PERMANENT GROUND DISPLACEMENT INDUCED BY SOIL LIQUEFACTION

(1) Procedure of analysis

This chapter deals with the response of a jointed pipeline subjected to permanent ground displacement. The mathematical analyses described in Chapter 3 is not available for jointed pipelines. Therefore, a modified transfer matrix method was used in this chapter[9]. The differences between the mathematical analysis shown in Chapter 3 and the simulation in this chapter are not only the type of pipelines but also the characteristics of equivalent soil spring constants, that is, linear model in Chapter 3 and bi-linear model in the present chapter. The bi-linear model used was shown in Fig. 8. This model is adopted for the seismic design standards for gas supply pipelines in Japan[10]. The pipelines used in the analysis were ductile pipelines, whose dimensions are also shown in Table 3. The model of the permanent ground displacement is the same as that presented in Chapter 3. The method described in this chapter is, of course, available for a continuous pipelines and tendency of the results obtained from simulations was similar to that in the preliminary mathematical analyses.

(2) Application of simulation models to existing pipelines

Fig. 9 and 10 show the results of the response simulations. These figures display the relationship between the maximum displacement angle at a joint and the width of the liquefied zone as shown in Fig. 6. Fig. 9 expresses the results for the non-liquefied superficial layer deformation, that is, $K_1/K_2=1.0$. It can be seen from Fig. 9 that the maximum displacement angle at a joint increases with a decrease in the width of the deformed ground. This tendency is identical to the results obtained in Chapter 3. Since the allowable value for displacement angle at a joint is 7°, failure at a joint can be caused by greater than 3 m

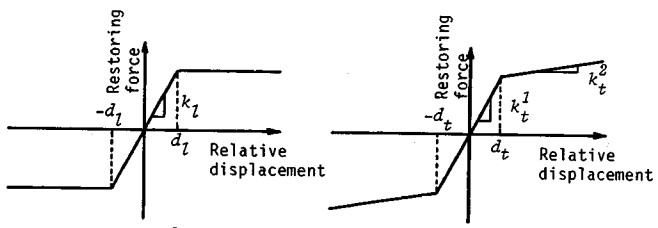

Fig. 8 Characteristic curves of equivalent soil spring constant.

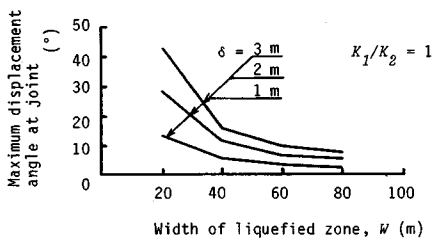

Fig. 9 Relationship between width of liquefied zone and maximum displacement angle at joint ($K_1/K_2=1$).

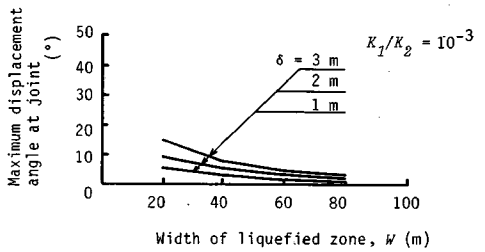

Fig. 10 Relationship between width of liquefied zone and maximum displacement angle at joint ($K_1/K_2=10^{-3}$).

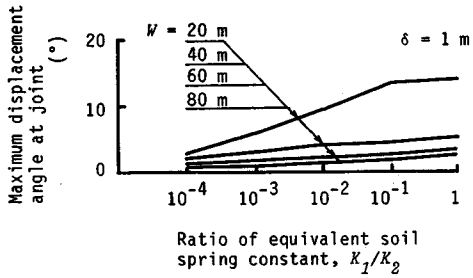

Fig. 11 Relationship between ratio of equivalent soil spring constant and maximum displacement angle at joint (δ=1 m).

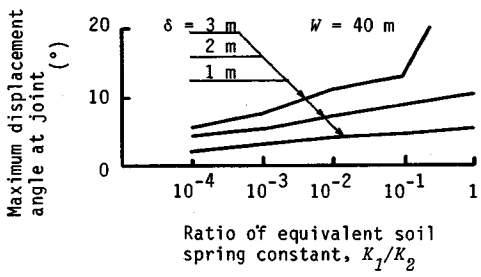

Fig. 12 Relationship between ratio of equivalent soil spring constant and maximum displacement angle at joint (W=40 m).

permanent ground displacement in an area less than 80 m. Pipe failure could also be caused by permanent ground displacement less than 1 m in an area less than 20 m. Fig. 10 shows the results for 10^{-3} of the ratio of equivalent soil spring constant, K_1/K_2. The maximum displacement angle at joints is smaller than that in Fig. 8, however, the tendency of lesser pipe response with increasing width of deformed ground is similar.

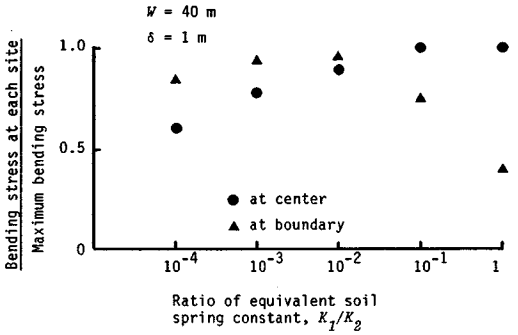

Fig. 13 Relationship between ratio of equivalent soil spring constant and ratio of bending stress to maximum bending stress.

Figs. 11 and 12 express the relationship between the maximum displacement angle at joints and the ratio of equivalent soil spring constant. Fig. 11 shows the response of pipelines in case of 1 m of the maximum magnitude of the permanent ground displacement and Fig. 12 reflects that in case of 40 m of width of deformed ground. It can be seen from these figures that the maximum displacement angle at a joint decreases with a decrease in the ratio of equivalent soil spring constant, that is, an increase of the degree of liqufaction. As shown in Fig. 3 in Chapter 2, permanent ground displacement in the liquefied ground is greater than that in the non-liquefied ground. This suggests that the greater the degree of liquefaction is, the greater the magnitude of the permanent ground displacement. For example, when the permanent ground displacement of 8 m, which was observed in Niigata City, occurs at the liquefied ground with 80 m width and 10^{-3} of the ratio of equivalent soil spring constant, the maximum displacement angle at joint becomes 15.1°. Therefore, the failure of pipes at joints could occur with even a relatively small ratio of equivalent soil spring constant, that is, great degree of liquefaction.

Fig. 13 reflects the ratio of bending stress to the maximum bending stress of the pipeline at the center of liquefied ground and at the boundary between liquefied and non-liquefied ground, respectively. According to this figure, the maximum bending stress occurs at the center of deformed ground in case of high ratio of equivalent soil spring constant, however, it appears at the boundary between the liquefied and non-liquefied areas in case of low ratio. This is also an interesting point.

The above results obtained by the response simulation seem to show that the probability of failure at joints is high for relatively narrow width of deformed non-liquefied superficial layer above the liquefied ground. Although we evaluate the response of pipelines subjected to permanent ground deformation, we do not take into consideration the relationship between the magnitude of the maximum ground displacement and the width of deformed ground in these examples. Since the experimental results obtained in Chapter 2 suggest that the width of deformed ground is one of the influential factors for the magnitude of the permanent ground displacement, it is crucial point to clarify this relationship between the magnitude of the

permanent ground displacement, the degree of liquefaction and the width of deformed ground quantitatively in the future.

5. CONCLUDING REMARKS

Through the experiments, mathematical analyses and response simulations, the following conclusions have been derived :

(1) According to the model experiments, a sinusoidal curve can be assumed as one of the distribution patterns of the permanent ground displacement perpendicular to the slope of ground. The relationship between the maximum ground displacement and width of the permanent ground displacement is indicated based on the experimental results. The findings suggest that the width of the liquefied area is one of the most influential factors determining the magnitude of the ground displacements.

(2) Formulae for pipeline response due to liquefaction-induced permanent ground displacement are proposed by using a beam theory. Application of the formulae reveals that the probability of failure is high for pipelines in areas with smaller width of the liquefied ground.

(3) The results of the response simulation for jointed pipelines suggest that the probability of failure at joints is high in areas where the deformed non-liquefied superficial layer above liquefied ground is with small width in case of the maximum permanent displacement exceeds 1 m.

(4) The relationship between the magnitude of permanent ground displacement, degree of liquefaction and width of deformed ground is one of the crucial points for evaluating the failure of pipelines subjected to permanent ground displacement.

(5) It is important to predict the liquefaction potential and generation of ground deformation in smaller extent for evaluating the pipelines' failure induced by permanent ground displacement.

Finally, we focused on only the response of the main distribution pipelines for water service with 400 mm nominal diameter to understand the response characteristics of the pipelines in this study, however, dimensionless parameters should be introduced to discuss the results quantitatively in the future analysis. Although the method for evaluation of pipeline response to permanent ground displacement induced by liquefaction was established in the present study, future study on the mechanisms of generation of permanent ground displacement is needed in order to clarify the effects of permanent ground displacement on pipelines.

ACKNOWLEDGEMENT

The authors wish to acknowledge Professor T. Kobori for his kind advise throughout the present study. This study is supported in part by the Grant-in-Aid for Scientific Research from the Ministry of Education, Science and Culture in Japan (No. 62750421). The calculation was performed by FACOM F-760 computer at the Information Processing Center, Kanazawa University.

REFERENCES

1) Hamada, M., Yasuda, S., Isoyama, R. and Emoto, K. : Observation of Permanent Ground Displacements Induced by Soil Liquefaction, Proc. of JSCE, No. 376, pp. 211-220, 1986 (in Japanese).

2) Hamada, M., Yasuda, S., Isoyama, R. and Emoto, K. : Study on Liquefaction-Induced Permanent Ground Displacements and Earthquake Damage, Proc. of JSCE, No. 376, pp. 221-229, 1986 (in Japanese).

3) Kitaura, M. and Miyajima, M. : Study on Behavior of Buried Pipelines due to Lateral Spreading Induced by Soil Liquefaction, Journal of Structural Engineering, JSCE, Vol. 33A, pp. 679-686, 1987 (in Japanese).

4) O'Rourke, T. D. and Tawfik, M. S. : Effects of Lateral Spreading on Buried Pipelines During the 1971 San Fernando Earthquake, Earthquake Behavior and Safety of Oil and Gas Storage Facilities, Buried Pipelines and Equipment, PVP-Vol. 77, ASME, pp. 124-132, 1983.

5) Yasuda, S., Tada, H., Fukusaki, S., Nakashima, R. and Yamamoto, Y. : Shaking Table Test of Liquefaction Induced Permanent Ground Displacement, Proc. of the 22nd Japan National Conference on Soil Mechanics and Foundation Engineering, pp. 731-734, 1987 (in Japanese).

6) Yoshida, T. and Uematsu, M. : Dynamic Behavior of a Pile in Liquefaction Sand, Proc. of the 5th Japan Earthquake Engineering Symposium 1978, pp. 657-663, 1987 (in Japanese).
7) Takada, S., Tanabe, K., Yamajyo, K. and Katagiri, S. : Liquefaction Analysis for Buried Pipelines, Proc. of the 3rd International Conference on Soil Dynamics and Eathquake Engineering, 1987.
8) Yasuda, S., Saito, K. and Suzuki, N. : Soil Spring Constant on Pipe in Liquefied Ground, Proc. of the 19th JSCE Conference on Earthquake Engineering, pp. 189-192, 1987 (in Japanese).
9) Kitaura, M., Miyajima, M. and Matsumura, Y. : Response Analysis of Buried Pipelines During Soil Liquefaction, Proc. of the 17 th JSCE Conference on Earthquake Engineering, pp. 303-306, 1983 (in Japanese).
10) Japan Gas Association : Recommended Practice for Earthquake Resistant Design of Gas Pipelines, pp. 177-182, 1982 (in Japanese).

(Received May 14 1988)